Available online at www.sciencedirect.com
SCIENCE DIRECT®
Applied Clay Science 31 (2006) 282–289
Applied CLAY Science
www.elsevier.com/locate/clay

Thermal and structural properties of Ca-rich Montmorillonite mechanically deformed by compaction and shear

Francesco Dellisanti [a], Vanna Minguzzi [a], Giovanni Valdrè [a,b,*]

[a] *Dipartimento di Scienze della Terra e Geo-Ambientali-Università di Bologna, Piazza di Porta S. Donato, 1 40126-Bologna, Italy*
[b] *Istituto Nazionale per la Fisica della Materia-Bologna, Italy*

Received 24 January 2005; received in revised form 5 August 2005; accepted 8 September 2005
Available online 28 November 2005

Abstract

This research work reports on the thermal and structural properties of powdered Ca-rich montmorillonite induced by mechanical deformation, which involves simultaneous compression and shear in a controlled thermodynamic environment. X-ray powder diffraction (XRPD), infra-red (FT-IR) and thermal analyses (TG-DTG-DTA) were employed for structural and thermal characterization.

Mechanical deformation performed up to 20 h induces significant physical and structural changes to Ca-rich montmorillonite as a function of time, leading to a progressive compaction and agglomeration of particles, reduction of crystallinity and an increase of microstrain, which affects both the tetrahedral and octahedral layers.

Thermal analysis of the deformed samples has indicated a loss of structural OH at a temperature which is well below the classical dehydroxylation temperature of the undeformed Ca-rich montmorillonite. This is a consequence of the disordered and defective structure (produced by the mechanical treatment), which requires a lower energy to induce the dehydroxylation of montmorillonite. Also the formation of mullite produced by heating montmorillonite at high temperature is affected by the mechanical treatment. The deformed samples yielded mullite with a faster kinetics at a lower temperature compared to their original counterparts (1155 instead of 1270 °C).

Keywords: Ca-rich montmorillonite; Thermal properties; Mechanical deformation; Medium–high temperature phases

1. Introduction

Bentonites are widely used in several industrial applications, such as foundries, petroleum drilling, civil engineering, catalysis, environmental remediation and animal feed, due to their high specific surface area, cation exchange capacity and swelling capacity related to the absorption of both water and organic molecules.

From the materials science point of view, montmorillonite and other clay minerals can be considered as natural nanostructured materials having size dependent properties. Recently, great attention has been paid to the study of structurally modified clay minerals after mechanical deformation via planetary ball milling because it induces physical and chemical changes in the treated materials that can be exploited either to enhance known properties, or for new application purposes. Most studies report the structural and textural changes of

* Corresponding author. Dipartimento di Scienze della Terra e Geo-Ambientali - Università di Bologna, Piazza di Porta S. Donato, 1 40126 - Bologna, Italy. Fax: +39 51 2094904.
E-mail address: gvaldre@geomin.unibo.it (G. Valdrè).

0169-1317/$ - see front matter © 2005 Elsevier B.V. All rights reserved.
doi:10.1016/j.clay.2005.09.006

kaolinite (Sanchez-Soto et al., 2000; Frost et al., 2001; Horváth et al., 2003), talc (Godet-Morand et al., 2002; Pérez-Maqueda et al., 2005), pyrophyllite (Pérez-Rodriguez et al., 1988) and montmorillonite (Čičel and Kranz, 1981; Christidis et al., 2004; Dellisanti and Valdrè, 2005). It was noted that the decrease of particle size can influence the thermal behaviour of kaolinite (Pérez-Rodriguez et al., 1992; Pérez-Maqueda et al., 1993; Sanchez-Soto et al., 2000; Franco et al., 2003; Horváth et al., 2003) and of pyrophyllite (Pérez-Maqueda et al., 1993; Pérez-Rodriguez et al., 1993). Such studies have also indicated that the thermal treatments of the deformed materials induce the formation of new crystalline and amorphous phases.

Since the literature is incomplete or lacks a detailed study on the thermal behaviour of Ca-rich montmorillonite deformed by compaction and shear, we have performed such an investigation, and here we report the results of a systematic thermal analysis of a Ca-rich montmorillonite modified by mechanical deformation at room temperature, in vacuum and in a well-defined and controlled thermodynamic environment. In a previous paper Dellisanti and Valdrè (2005) reported the structural properties of a Ca-rich montmorillonite after mechanical treatment. In this work we discuss in particular the formation of medium and high-temperature phases in relation to the different degree of mechanical deformation of Ca-rich montmorillonite.

2. Experimental

2.1. Materials and thermal analysis

Commercial powdered Ca-bentonite samples (Laviosa SpA, Livorno, Italy) of about 25 μm average grain size were mechanically deformed for 1 and 20 h (hereinafter named 1-h and 20-h, respectively) via a specifically home-modified planetary ball mill working at room temperature and under medium/high-vacuum of 0.13 Pa (10^{-3} Torr) using hardened steel balls (Bonetti et al., 1998). This mechanical apparatus induces simultaneous compaction and shear in the material in controlled thermodynamic environment, whereas the dynamic vacuum treatment increases the transformation efficiency, as described by Dellisanti and Valdrè (2005). The bentonite consists of Ca-rich montmorillonite (>90%) and other minor phases represented by opal CT and feldspars. The mechanically untreated material (i.e., the starting bentonite) is in the following named 0-h.

The thermal behaviour of both untreated (0-h) and deformed montmorillonite (1-h; 20-h) was studied with a Setaram Labsys double furnace apparatus with simultaneous recording of thermogravimetric (TG) and differential thermal analysis (DTA) data. Thermal analysis was performed in the range 20 to 1300 °C with a heating rate of 10 K/min, using about 60 mg of material/sample, platinum crucibles, calcined Al_2O_3 as reference substance, a flow rate of helium of 0.27 ml/s. The temperature accuracy is about ±1 °C.

2.2. Methods

2.2.1. X-ray powder diffraction

Mineralogical and crystallographical data of the original (0-h) and the deformed samples (1-h and 20-h) were obtained by powder X-ray diffraction (XRD). Analyses were performed by using a Philips PW 1710 diffractometer equipped with a graphite monochromator using CuKα radiation, 40 kV and 30 mA power supply, 1° divergence and detector slits, 0.02° (2θ) step size and a counting time of 10 s/step. XRD patterns were collected from 3° to 65° (2θ).

The deformed samples were prepared by side filling an aluminium holder in order to obtain a quasi-random orientation. In addition, further XRD analyses were performed on the <2 μm fraction after sedimentation from suspension (Christidis et al., 2005). The dispersion was performed in distilled water using an ultrasonic probe (20 s). No change of diffraction patterns of the materials after the two preparation methods were observed.

2.2.2. Infra-red spectroscopy

Infra-red spectra were obtained with a Nicolet Avatar 360 Fourier Transform Infra Red (FT-IR) spectrometer. All spectra were collected under the following conditions: spectrum range from 4000 to 400 cm^{-1}, spectral resolution of 4 cm^{-1} and 64 accumulations per spectrum. A mixture of about 1 mg of sample and 200 mg of KBr was prepared to obtain pellets of 13 mm diameter at a pressure of 8 metric tons/cm^2 in a specific die. Before analysis the pellets were heated overnight at 150 °C to remove adsorbed water.

3. Results and discussion

3.1. Mechanical treatment

After mechanical treatment, the Ca-rich montmorillonite shows a progressive removal of interlayer water molecules and structural destabilization of structural OH as a non-linear function of treatment time (Dellisanti and Valdrè, 2005). In particular, the 20-h samples display remarkable decrease and broadening of the (*00l*) and (*0k0*) diffraction peaks (Fig. 1), indicating a progressive reduction of structural order and an increase of microstrain. Furthermore, the 001 peak migrates to lower d-spacings indicating a variable degree of hydration of the smectite layers. The peak is centered at 6.6° 2θ (1.34 nm), which suggests predominance of partially hydrated layers. Another interesting result is the lack of amorphization in the treated material. In fact, there is no increase of XRD

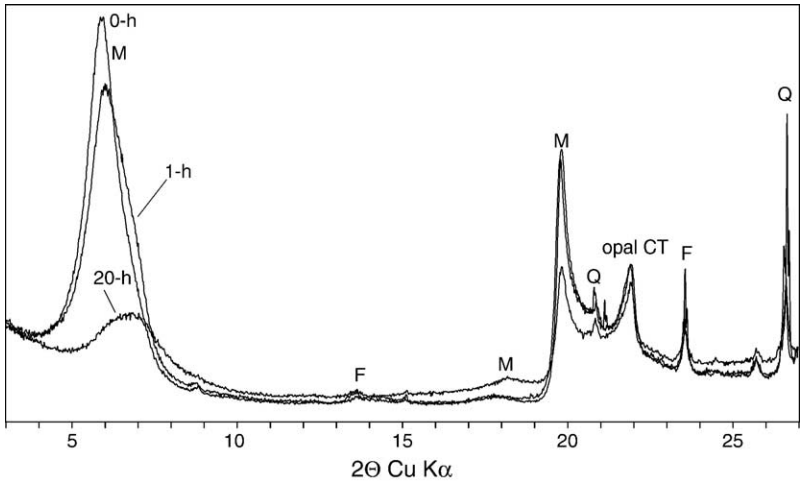

Fig. 1. Comparison between XRD pattern before (0-h) and after mechanical treatments (1-h and 20-h) of Ca-rich montmorillonite (M). Q: quartz (internal standard); F: feldspars (from Dellisanti and Valdrè, 2005 modified).

background in the 2θ range 20–30° as shown in Fig. 1. Generally, the use of conventional ball or planetary mills yields almost totally amorphous material after 20 h of grinding (Volzone et al., 1987). On the contrary, our apparatus does not produce amorphous material, but seems to break montmorillonite crystallites along the *ab* plane during the first stage of milling. After prolonged milling up to 20-h a structural destabilization in the *ac* or *bc* planes starts to occur, associated with re-aggregation (cold-welding according to Gregg, 1968) as reported by Dellisanti and Valdrè (2005). FT-IR data (Fig. 2) show an intensity decrease and broadening of 866 cm^{-1} band (Al–Fe^{3+}–OH vibration), 633 cm^{-1} band (Al–O–Al vibration, Farmer and Russel, 1964) and 522 cm^{-1} band (Si–O–Al vibrations) indicating bond breaking and disordering within the octahedral and between the tetrahedral and octahedral sheets of Ca-rich montmorillonite. Powder laser diffraction analysis (Dellisanti and Valdrè, 2005) has showed agglomeration and compaction of particles after 20 h of deformation. In accordance, BET analysis (Brunauer et al., 1938) indicated a reduction of the specific surface area from 37 ($m^2\ g^{-1}$) of the 0-h sample to 32 ($m^2\ g^{-1}$) of the sample deformed for 20 h. However, a detailed comparison of absorption properties of deformed montmorillonites will be presented in forthcoming papers (Christidis et al., 2005).

3.2. Thermal analysis

Results from thermal analysis are reported in Figs. 3 and 4. In Fig. 3 the TG curve of the original sample (0-h) shows three main steps of weight loss. In the first step ($T<200$ °C) a weight loss (about 7%)

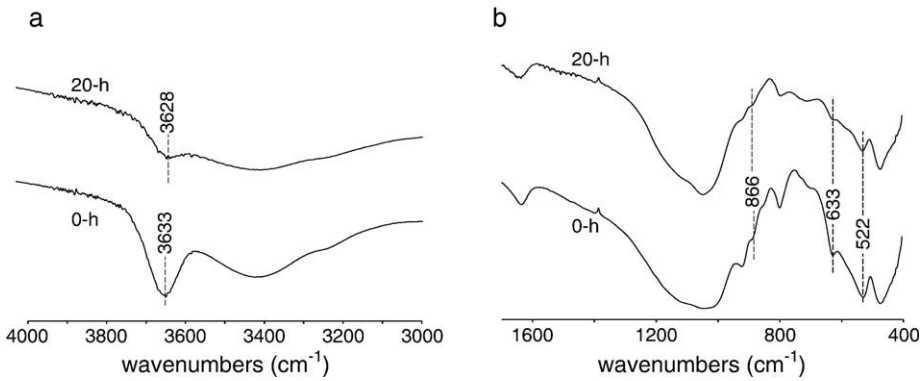

Fig. 2. FT-IR spectra of 0-h and 20-h samples of Ca-rich montmorillonite: (a) 4000–3000 cm^{-1} range; (b) 1700–400 cm^{-1} range (from Dellisanti and Valdrè, 2005 modified).

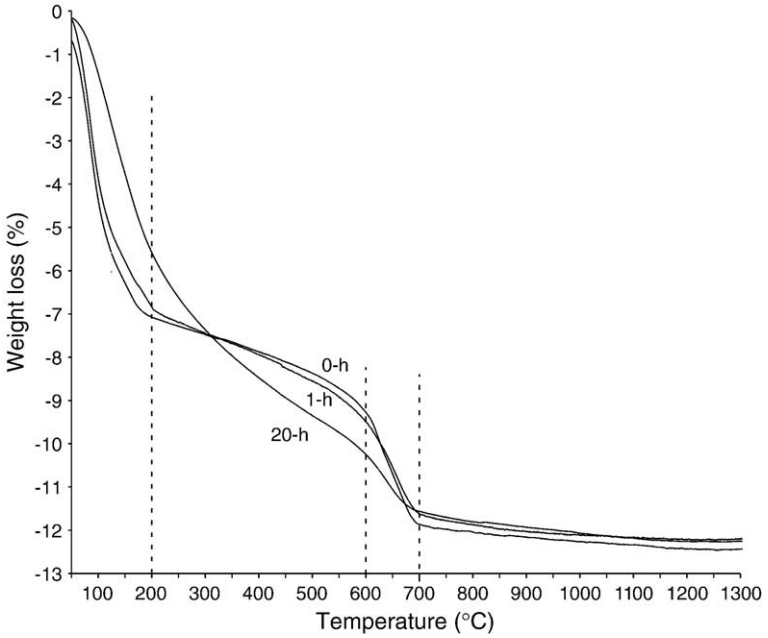

Fig. 3. Comparison between TG curves up to 1300 °C before (0-h) and after mechanical treatments (1-h and 20-h) of Ca-rich montmorillonite.

corresponding to both adsorbed and interlayer water loss takes place. After this step, the TG curve shows a slight gradual decrease (about 2%) in the range 200–600 °C, which is attributed to the water loss of both Ca-rich montmorillonite and opal CT present in the sample. Finally, a third main loss occurs at temperatures in the range 600–700 °C, where the TG curve displays a steep weight loss (about 3.5%) related to the release of structural OH of Ca-rich montmorillonite. The dehydroxylation temperature of about 680 °C (see Fig. 4) is in agreement with the classical range of dehydroxylation temperature (600–700 °C) observed by various authors for *cis*-vacant montmorillonites (Tsipursky and Drits, 1984; Drits et al., 1995). The total weight loss at 1300 °C is about 12.5% (Fig. 3).

The thermal behaviour of the samples deformed for 1 h (1-h) is very similar to the untreated one (Fig. 3); also the weight losses in the above mentioned three main steps, are similar.

In the sample deformed for 20 h (20-h) a different thermogravimetric behaviour was observed (Fig. 3). The TG curve can be generally described by two main steps of weight loss. In the first step ($T<600$ °C) a slow monotonic weight loss (up to about 10.5%) takes place. This weight loss is attributed to four different processes:

i) Loss of adsorbed water (usually released up to 100 °C);
ii) Loss of interlayer water (released from 100 to 250 °C);
iii) Loss of water from Ca-rich montmorillonite and opal CT (released from 200 to 600 °C), and simultaneously;
iv) Loss of OH of a defective montmorillonite phase (produced by the mechanical deformation) released continuously up to 600 °C. The water loss in this region suggests that dehydroxylation begins before all adsorbed water has been removed.

Mechanical deformation destroys the structure of Ca-rich montmorillonite between tetrahedral and octahedral layers (as shown by XRD and FT-IR) and induces a release of structural OH at temperature lower than 600 °C, probably starting before 300 °C as suggested by the first intersection of the three integral TG curves reported in Fig. 3. Before this intersection the TG curve of the 20-h shows a lower weight loss than that of 0-h and 1-h. On the contrary, after 300 °C the TG curve of the 20-h shows a higher weight loss than that of 0-h and 1-h. This indicates an additional contribution to the weight loss of the 20-h sample starting at the temperature of about 300 °C. Since the final total weight loss is practically the same for 0-h, 1-h and 20-h samples (ca. 12.5%), we can hypothesize that the additional contribution may come from an anticipated dehydroxylation of

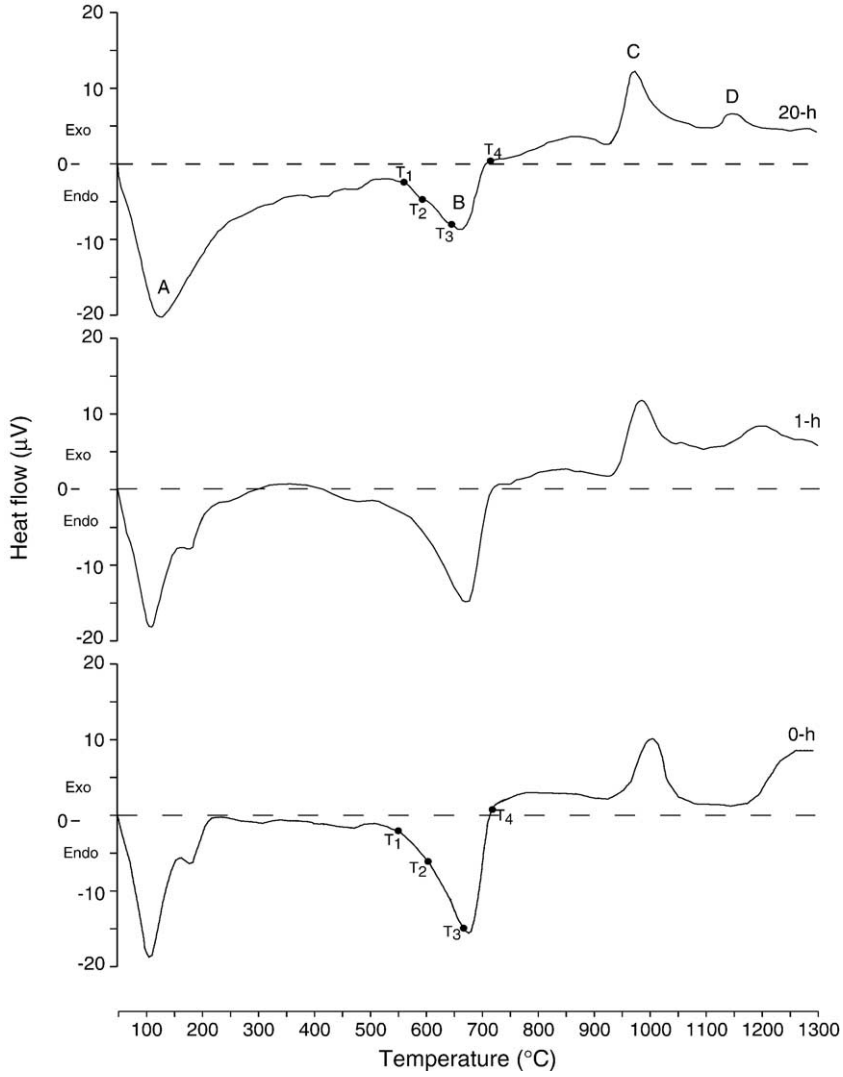

Fig. 4. Comparison between DTA curves up to 1300 °C before (0-h) and after mechanical treatments (1-h and 20-h) of Ca-rich montmorillonite. T_1, T_2, T_3 and T_4 are temperatures at which isothermal analyses were performed (see text for details).

deformed Ca-rich montmorillonite, which takes place at a lower temperature than that for 0-h sample. This anticipated dehydroxylation could be related to a change of the geometry of the octahedral sheet into a *trans*-vacant configuration produced by the mechanical deformation of a starting *cis*-vacant montmorillonite.

The second step of main loss of the 20-h sample occurs at temperatures between 600–700 °C, where the TG curve displays a weight loss (about 2%) related to the classical dehydroxylation of the structural OH of a remaining undefective *cis*-vacant Ca-rich montmorillonite. In fact, as can be seen from the DTA curve of Fig. 4, the classical dehydroxylation temperature is 665 °C. For the 20-h samples in the temperature range 600–700 °C the TG curve behaves similarly to that 0-h sample. However, note that in this temperature range (600–700 °C) the 0-h sample displays 3.5% of weight loss instead of the 2% of 20-h.

In conclusion, the 20-h Ca-rich montmorillonite sample looses the structural OH in two different steps:

i) Continuously at temperatures well below 600 °C from a defective montmorillonite structure, and
ii) In the range 600–700 °C with a similar trend of undefective montmorillonite.

The thermal analysis has indicated that the mechanical deformation of Ca-rich montmorillonite after

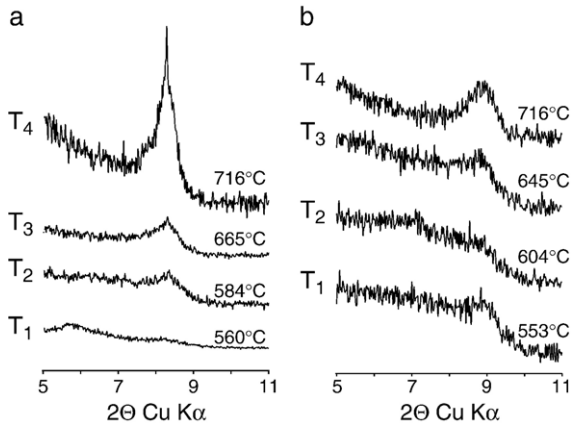

Fig. 5. XRD patterns of 0-h and 20-h after heating in isothermal mode at four temperatures (see Fig. 4). (a) 0-h (001) basal diffraction peak; (b) 20-h (001) basal diffraction peak.

20 h has not completely destroyed the structure of montmorillonite corroborating the XRD and FTIR results.

The fact that for temperatures less than 300 °C, the 20-h sample displays a weight loss lower than that of 0-h and 1-h samples can be explained by the higher particles agglomeration and compaction of 20-h samples, as was observed by laser diffraction analysis (Dellisanti and Valdrè, 2005); consequently they reduce and delay the desorption of both adsorbed and interlayer water.

The general trend of the DTA curves of 0-h, 1-h, 20-h samples (Fig. 4) shows the presence of endothermic reactions (indicated as A) due to the loss of interlayer and adsorbed water (at temperatures up to about 200–250 °C) and to the dehydroxylation reaction (B) of Ca-rich montmorillonite between 650 and 700 °C. These losses are more pronounced in the 0-h and 1-h samples, whereas the 20-h sample presents a generally more broadened and less intense reactions because of the defective material induced by mechanical deformation.

These observations are in agreement with Čičel and Kranz (1981), although they deformed the montmorillonite only by percussive grinding. It is also in line with similar observations of kaolinite and talc (Horváth et al., 2003; Dellisanti et al., 2004).

After the reaction B, the thermal heating produces in all samples one clear exothermic peak C in the range 950–1050 °C still not completely understood but probably attributable to the rearrangement of high-temperature silica phases (Čičel and Kranz, 1981). Finally, an exothermic reaction (D) occurs due to the recrystallization of mullite, as indicated by XRD (Fig. 6). In fact, the DTA curve of Fig. 4 shows broad exothermic peaks D relative to the formation of mullite for 0-h (T=1270 °C) and 1-h (T=1210 °C) samples; in the 20-h sample the same peak is sharper and is observed at about 100 °C lower (T=1155 °C) than that of 0-h and 1-h samples (Fig. 4), indicating that in the 20-h samples the kinetics of mullite crystallization is more pronounced and faster.

3.3. XRD data after isothermal treatment

In order to study the effect of mechanical deformation on the 001 basal peak of montmorillonite in the vicinity of the classical dehydroxylation temperature (point B of Fig. 4), we have performed XRD analyses after isothermal heating (for 2 h) at various temperatures close to the maximum of dehydroxylation (as indicated in Fig. 4). Four temperature were chosen: T_1, at the beginning of the dehydroxylation; T_2, at an intermediate temperature of the reaction; T_3, very close to the temperature of the maximum of dehydroxylation, and T_4, at the end of the dehydroxylation reaction. The isothermal gravimetric behaviour of montmorillonite dehydroxylation will be reported in a future paper where the kinetics of the reaction and the activation energy will be given.

Fig. 5a shows XRD traces for the 0-h sample. At 560 °C a peak relative to a layered structure with a basal plane spacing of 1.0 nm begins to appear (Table 1). In fact, at 560 °C the montmorillonite structure may not be collapsed and this can explain the XRD peak at about 6° (2θ) present in Fig. 5a. At 584 °C montmorillonite has lost interlayer water,

Table 1
Mineralogical and crystallographic parameters relative to the (001) basal peak of isothermally heated samples for 2 h; n.d. data not detectable

T (°C)	Peak position (2θ CuKα)	d(001) (nm)	FWHM (Δ° 2θ)
0-h sample			
560	8.85	1.0	0.97
584	8.92	1.0	0.58
665	8.92	1.0	0.55
716	8.85	1.0	0.44
20-h sample			
553	8.93	1.0	0.79
604	n.d.	n.d	n.d.
645	8.87	1.0	0.78
716	8.98	1.0	0.67

correspondingly the (001) basal plane spacing shrinks from 1.5 to about 1.0 nm. At 665 °C the FWHM (full width at half maximum) of the (001) basal plane decreases and finally at 716 °C, the peak is further sharpened (Table 1).

In sample 20-h, heating at 553 °C produces a decrease of basal spacing from 1.3 to 1.0 nm attributable to the removal of interlayer water. In the sample heated up to 645 °C the FWHM of the basal plane spacing starts to decrease (Fig. 5b and Table 1). After the treatment at 716 °C a sharp symmetric peak is clearly visible but the value of the FWHM is higher in comparison to that of 0-h sample at the same temperature (Table 1).

These results indicate that mechanical deformation could induce modifications to the montmorillonite basal plane spacing and FWHM in the temperature range 200–700 °C.

3.4. XRD data for samples heated up to 1300 °C

Samples 0-h and 20-h heated at 1300 °C show very similar XRD patterns with recrystallization of mullite as a high temperature phase (Fig. 6). However, mullite recrystallization in the 20-h deformed sample takes place at about 1155 °C, which is 115 °C lower than for untreated one (1270 °C), according to the DTA data (see reaction D in Fig. 4). In addition, the 20-h sample presents more intense and sharp XRD peaks of mullite than 0-h sample. These two effects have been attributed to the concomitant presence of a high degree of structural disorder in the montmorillonite and to the reduction of the crystallite size caused by mechanical treatment (Dellisanti and Valdrè, 2005); consequently the deformed material has a higher reactivity than the untreated sample.

A glassy phase is also present in the 20-h sample heated at 1300 °C, indicated by a broad X-ray peak in the range between 20° and 30° (2θ CuKα).

4. Conclusions

The present investigation clearly shows that both structural and thermal properties of Ca-rich montmorillonite can be significantly influenced by mechanical deformation (simultaneous compaction and shear) at room temperature in vacuum. An interesting result of our method of mechanical deformation is the lack of amorphization in the treated Ca-rich montmorillonite in comparison with conventional ball or planetary mills.

This kind of mechanical deformation of Ca-rich montmorillonite leads to a progressive removal of interlayer water molecules and a structural destabilization of intralayer OH with increasing the time of treatment. The structural disorder produced by deformation facilitates the dehydroxylation with respect to the untreated materials. In fact, the structural OH weight loss takes place at temperatures lower than those for undeformed material. It is analogous to that observed for other clay minerals such as kaolinite and talc.

The high temperature thermal recrystallization of mullite in deformed Ca-rich montmorillonite takes place at a lower temperature (1155 °C of 20-h samples instead of 1270 °C of 0-h samples) and is faster than for the untreated materials.

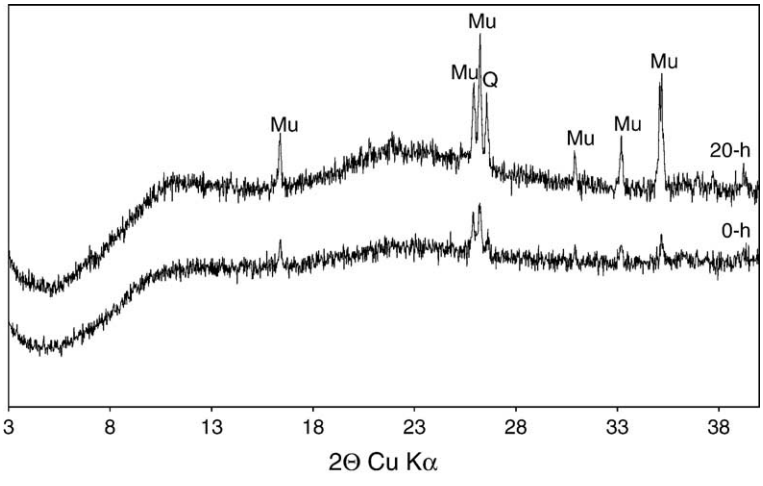

Fig. 6. Comparison between XRD patterns of 0-h and 20-h deformed samples after heating at 1300 °C. Mu: mullite; Q: quartz (internal standard).

Acknowledgement

Project funded by "Finanziamenti Pluriennali 2002", University of Bologna.

References

Bonetti, E., Campari, E.G., Pasquini, L., Sampaolesi, E., Valdrè, G., 1998. Structural and elastic properties of nanocrystalline iron and nickel prepared by ball milling in controlled thermodynamic environment. Materials Science Forum 269–272, 1005–1010.

Brunauer, S., Emmet, P.H., Teller, E., 1938. Adsorption of gases in multimolecular layers. Journal of the American Chemical Society 60, 309–319.

Christidis, G.E., Makri, P., Perdikatsis, V., 2004. Influence of grinding on the structure and colour properties of talc, bentonite and calcite white fillers. Clay Minerals 39/2, 163–175.

Christidis, G.E., Dellisanti, F., Valdrè, G., Makri, P., 2005. Structural modifications of smectites mechanically deformed under controlled conditions. Proceedings XIII International Clay Conference. Tokio 20–27 August 2005. Accepted in extended version to Clay Minerals.

Čičel, B., Kranz, G., 1981. Mechanism of montmorillonite structure degradation by percussive grinding. Clay Minerals 16, 151–162.

Dellisanti, F., Valdrè, G., 2005. Study of structural properties of ion treated and mechanically deformed commercial bentonite. Applied Clay Science 28, 233–244.

Dellisanti, F., Minguzzi, V., Valdrè, G., 2004. Structural, thermal and surface force characterization of modified layer silicates: results on talc, kaolinite and montmorillonite. Acta Mineralogica-Petrographica, Abstract Series 4, 26.

Drits, V.A., Besson, G., Muller, F., 1995. An improved model for structural transformations of heat-treated aluminous dioctahedral 2:1 layer silicates. Clays and Clay Minerals 43/6, 718–731.

Farmer, V.C., Russel, J.D., 1964. The infra-red spectra of layer silicates. Spectrochimica Acta 20, 1149–1173.

Franco, F., Pérez-Maqueda, L.A., Pérez-Rodriguez, J.L., 2003. The influence of ultrasound on the thermal behaviour of a well ordered kaolinite. Thermochimica Acta 404, 71–79.

Frost, R.L., Mako, E., Kristof, J., Horvath, E., Kloprogge, J.T., 2001. Mechanochemical treatment of kaolinite. Journal of Colloid and Interface Science 239/2, 458–466.

Godet-Morand, L., Chamayou, A., Dodds, J., 2002. Talc grinding in an opposed air jet mill: start-up, product quality and production rate optimisation. Powder Technology 128, 306–313.

Gregg, S.J., 1968. Surface chemical study of comminuted and compacted solids. Chemistry and Industry 11, 611–617.

Horváth, E., Frost, R.L., Makò, E., Kristòf, J., Cseh, T., 2003. Thermal treatment of mechanochemically activated kaolinite. Thermochimica Acta 404, 227–234.

Pérez-Maqueda, L.A., Pérez-Rodriguez, J.L., Scheiffele, G.W., Justo, A., Sanchez-Soto, P.J., 1993. Thermal analysis of ground kaolinite and pyrophyllite. Journal Thermal Analysis 39, 1055–1067.

Pérez-Maqueda, L.A., Duran, A., Pérez-Rodríguez, J.L., 2005. Preparation of submicron talc particles by sonication. Applied Clay Science 28, 245–255.

Pérez-Rodriguez, J.L., Madrid, L., Sanchez-Soto, P.J., 1988. Effects on dry grinding on pyrophyllite. Clay Minerals 23, 399–410.

Pérez-Rodriguez, J.L., Pérez-Maqueda, L.A., Justo, A., Sanchez-Soto, P.J., 1992. Influence of grinding contamination on high temperature phases of kaolinite. Industrial Ceramic 12, 109–113.

Pérez-Rodriguez, J.L., Pérez-Maqueda, L.A., Justo, A., Sanchez-Soto, P.J., 1993. Influence of grinding contamination on high temperature phases of pyrophyllite. Journal European Ceramic Society 11, 335–339.

Sanchez-Soto, P.J., Jimenez de Haro, M.C., Pérez-Maqueda, L.A., Varona-Vaira, I., Pérez-Rodríguez, J.L., 2000. Effect of dry grinding on the structural changes of kaolinite powders. Journal American Ceramic Society 83, 1649–1657.

Tsipursky, S.I., Drits, V.A., 1984. The distribution of octahedral cations in the 2:1 layers of dioctahedral smectites studied by oblique texture electron diffraction. Clay Minerals 19, 177–192.

Volzone, C., Aglietti, E.F., Scian, A.N., Porto Lopez, J.M., 1987. Effect of induced structural modifications on the physicochemical behaviour of bentonite. Applied Clay Science 2, 97–104.